A&A manuscript no.
(will be inserted by hand later)

Your thesaurus codes are:
09.02.1, 09.19.1, 11.09.4, 11.09.5, 11.13.1, 13.21.3

ASTRONOMY
AND
ASTROPHYSICS
1.2.2008

C IV absorption from hot gas inside supergiant shell LMC 4 observed with HST and IUE ⋆

D.J. Bomans[1,2,⋆⋆], K.S. de Boer[1], J. Koornneef[3], and E.K. Grebel[1,4]

[1] Sternwarte der Universität Bonn, Auf dem Hügel 71, D-53121 Bonn, Federal Republic of Germany
[2] University of Illinois, Dept. of Astronomy, 1002 West Green St., Urbana, IL 61801, U.S.A.
[3] SRON Laboratory for Space Research, Postbus 800, NL-9700AV Groningen, The Netherlands
[4] Space Telescope Science Institute, 3700 San Martin Drive, Baltimore, MD 21218, U.S.A.

received 21 Nov. 1995; accepted 11 Jan. 1996

Abstract. High resolution ultraviolet spectra with HST-GHRS of two stars in the direction of the supergiant shell LMC 4 unambiguously show absorption by substantial quantities of C IV gas at velocities near the the systemic velocity of the LMC. In combination with the detection of diffuse X-rays from the LMC 4 by ROSAT and other supporting data, this demonstrates that the interior of LMC 4 is filled with tenuous hot gas.
C IV interstellar absorption is seen over a large velocity range, having at least 2 components at about 280 and 320 km s^{-1}. The strong component at 280 km s^{-1} has a width of 40 km s^{-1} and a column density in the order of 3 10^{13} cm^{-2}. The width of the absorption is best explained by bulk motions of C IV-containing gas clouds inside LMC 4. These hot clouds or layers around cold clouds have to have a relatively high filling factor inside LMC 4 to fit the observations. The characteristics of the C IV gas component at 320 km s^{-1} are such that they trace a blast wave from a recent supernova within the LMC 4 cavity.
Galactic C IV absorption is also present, as to be expected for these lines of sight.

Key words: ISM: bubbles – ISM: structure – Galaxies: ISM – Galaxies: irregular – Magellanic Clouds – Ultraviolet: ISM

1. Introduction

Supergiant shells are important features in the overall structure of a number of starforming galaxies [1]. Typically, they are outlined by numerous diffuse and often filamentary HII regions which provide evidence for recent star formation at the interface between the shell and the ambient interstellar medium. The ionized shell encloses a space which contains remarkably little warm and/or cold gas (for LMC 4 see the HI map in Rohlfs et al. 1984, and the CO map in Cohen et al. 1988). In the Large Magellanic Cloud (LMC) several such structures are known (Goudis & Meaburn 1978, Meaburn 1980). Of these, the supergiant shell LMC 4 is the largest with a diameter of over 1.2 kpc.

A clear connection between the existence of supergiant shells and active starformation has been established (see e.g. Deul & den Hartog 1990, Hunter et al. 1993), but models explaining the origin of the largest of these structures are still lacking. While the combination of winds from hot, young stars and the blasts from supernova (SN) explosions from a single starburst event (e.g. Mac Low et al. 1989) appears adequate to produce the smaller shells, this model fails for the largest structures (e.g. Igumentshchev et al. 1990). Adding the effects of self-propagating star formation to the overall energy input may provide a way to create objects like LMC 4 but has not yet been thoroughly modelled. However, if the supershells were due to radially propagating star formation, the young stellar associations and H II regions that define the shell would be expected to surround an interior containing older stars. Observationally, the observed age structure of various stellar groups in LMC 4 (see Vallenari et al. 1993, Bomans et al. 1994, Bomans et al. 1995, and Domgörgen et al. 1995 for discussions) does not appear to match this prediction. A further complication is that the size of the supershells exceeds the

Send offprint requests to: D.J. Bomans, USA address, email: bomans@astro.uiuc.edu

⋆ Based on observations obtained with the NASA/ESA *Hubble Space Telescope* obtained at the Space Telescope Science Institute, which is operated by AURA Inc. under NASA contract NAS 5-26555; and with the IUE satellite from VILSPA, Spain, jointly operated by the NASA, ESA, and PPARC

⋆⋆ Feodor Lynen fellow of the Humboldt Foundation

[1] Large shell structures have now been identified in at least 30 nearby galaxies (see e.g. Bomans 1994).

scale height of a typical galaxy. Therefore, blow-out – i.e., mass and energy loss into the halo – is critical for the understanding of these structures. Hydrodynamical simulations of astrophysical plasmas (e.g. Suchkov et al. 1994) are consistent with the observation that little neutral or low-ionized gas exists within the supergiant shells, but require a hot and highly ionized component It is this gas that we have been trying to definitively establish trough its absorptions in the ultraviolet.

A first indication for the presence of highly ionized gas in the LMC was found by Koornneef et al. (1979) and de Boer et al. (1980) in high resolution spectra obtained with the International Ultraviolet Explorer (IUE) satellite. Absorption by C IV was present in many directions indicating the presence of a halo of coronal gas around the LMC (de Boer & Savage 1980). In particular, the presence of C IV absorption in spectra of HD 36402 in the general direction of LMC 4 (de Boer & Nash 1982) suggested the existence of gas of at least 10^5K. On the basis of the observations on this line of sight, a pressure of $nT = 2\,10^4$ cm^{-3} K was computed for gas inside LMC 4 . However, HD 36402 is located at the edge of LMC 4 within a distinct structure (the giant, 100 pc diameter, shell N 51D), allowing the possibility that this C IV absorption had a more local origin. A more recent observation by Chu & Mac Low (1990) shows that the inside of the nebula N 51D is bright in soft X-rays, thus confirming the existence of a very hot and highly ionized component.

A more definitive search for C IV absorptions in LMC 4 should therefore rely on the observations of stars whose lines of sight intersect the bubble closer to its center. The number of targets satisfying this criterion is very limited, and additional requirements are to be put on the spectral types of the stars. A high UV continuum flux is needed to provide a sufficient signal to noise ratio, but the stars should not be so hot as to produce significant amounts of circumstellar C IV. This limits the optimal targets to luminous stars, preferably in the spectral types to O9 to B2. Given these constraints, we selected stars inside LMC 4 for our intended science program and added a few more stars observed with IUE for different programs. The stars are listed in Table 1.

Initially we relied on the IUE (Boggess et al. 1978) to acquire ultraviolet spectra, with the first observations scheduled in 1986. We found the resulting data extremely useful for various reasons (Section 8 and Bomans et al. 1990, Domgörgen et al. 1993), but due to the limited collecting area and the restricted signal to noise ratio achievable with IUE, we could not convince ourselves that the data were adequate to yield reliable column densities for a hot gas component inside LMC 4. We therefore decided to observe a subset of the IUE targets, for limited range of wavelengths, with the Goddard High Resolution Spectrograph (GHRS) on the Hubble Space Telescope (HST). The data were obtained on 1 July 1993 and 26 December 1993, i.e. before the installation of COSTAR.

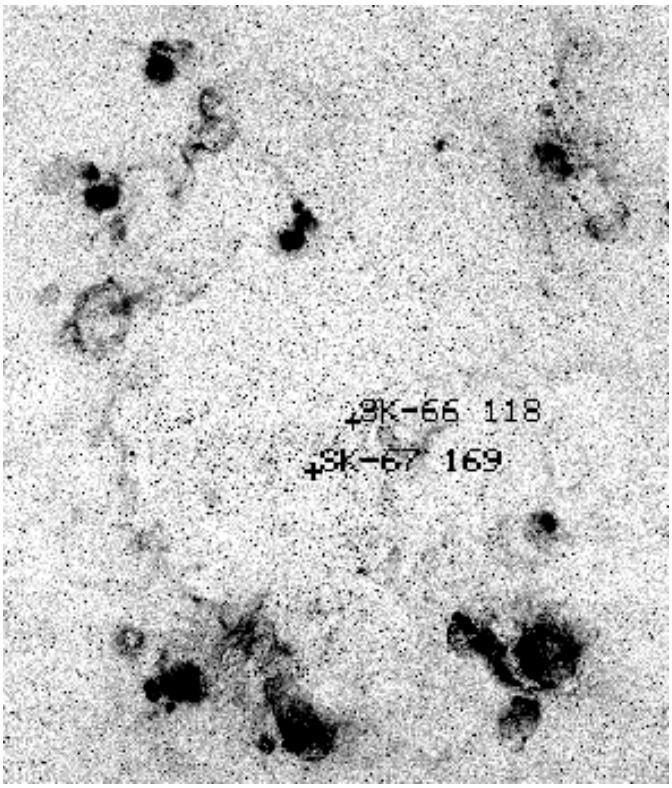

Fig. 1. Hα image of supergiant shell LMC 4 made from a scan of a photographic plate taken with the Curtis Schmidt telescope at Cerro Tololo (Kennicutt & Hodge 1986). The location of the HST target stars are marked with plus signs.

While the analysis of our HST data was ongoing, we detected significant amounts of X-ray emission from the inside of LMC 4 with ROSAT (Bomans et al. 1994). Previous X-ray satellites had produced data in which diffuse soft X-ray emission seemed to be discernible from the general area of LMC 4, but that radiation was too weak and the measurements were too noisy to establish proof (see discussion by Bomans et al. 1994). Also, Chu et al. (1994) detected significant amounts of C IV absorption associated with the supergiant shell LMC 3. Their data are taken from an IUE survey for high velocity C IV absorption, and the relatively easy detection of C IV in LMC 3 contrasts with our difficulty of firmly establishing this component in LMC 4 using the same instrumentation. While some of the stars in the Chu et al. (1994) survey are quite hot, and might have produced some circumstellar C IV, the possibility that the physical conditions within the two largest LMC supergiant shells are different clearly arises. Any models for the supershells would then have to explain the variation in these absorptions between otherwise quite similar systems.

In the present paper we discuss the results from our spectroscopic observations toward two stars inside LMC 4 with the HST, and from five stars inside LMC 4 as observed with the IUE. The location of the stars observed

Table 1. Data on the target stars

Star	RA	DEC	V	Sp.T.	IUE	HST
Sk −66 117	5 30 36	−66 49	12.68	B3 I	y	n
Sk −66 118	5 30 54	−66 55	11.81	B2 Ia[a]	y	y
Sk −66 100	5 27 49	−66 58	13.26	O6 Ib[c]	y	n
Sk −67 206	5 34 48	−67 03	12.00	BN0.5 Iaw[a]	y	n
Sk −67 169	5 31 54	−67 04	12.18	B1 Ia[a]	y	y
Sk −67 166	5 31 50	−67 40	12.27	O4 If+[b]	y	n

Spectral types are from: [a]Fitzpatrick (1988), [b]Walborn (1977), [c]Conti et al. (1986)

with HST is indicated in a sketch of the region (Fig. 1), for the others we refer to Domörgen et al. (1995). The actual data and reduction procedures will be described in section 2, while in section 3 we briefly discuss the stellar features in the HST spectra as far as they are relevant to the analysis of the interstellar absorption features. In section 4 we turn to the low ionized gas, while in section 5 we derive information about C IV from the spectra. Section 6 describes the spectral restoration algorithm adopted, as well as the results derived from the spectra processed in this manner. Section 7 introduces an analysis technique which involves profile fitting. Results thereof are then compared with those of sections 5 and 6, and provide a useful cross check. A confrontation between the HST results and those from IUE is provided in section 8. Finally, section 9 is devoted to a discussion of the consequences of our observations.

2. Observations and data reduction

We used the Goddard High Resolution Spectrograph (GHRS) aboard the Hubble Space Telescope (HST) to take spectra of Sk −67 169 and Sk −66 118 in two spectral ranges each. We selected these two stars, because the IUE high dispersion spectra prove that the stars are located inside LMC 4 and their projected location in the very center of LMC 4 should provide the largest path-length through the supergiant shell.

The technical data of those four HST observations are summarized in Table 2. The two wavelength ranges chosen contain a large number of interstellar absorption lines representing gas of quite different ionization properties. In the spectral region from 1530 to 1570 Å lines of C IV and of C I, C I*, and C I** are expected, while in the spectral range from 1285 to 1325 Å absorption lines of O I, Si II, O I*, Ni II are located. C I represents the neutral gas where the lines from the excited levels sample the densest parts of that gas. Si II and O I sample normal neutral gas and, due to the relatively large intrinsic optical depth of the transitions, also the more dilute portions. Ni II traces the densest parts of the neutral gas. C IV in absorption represents the presence of highly ionized and hot gas.

The aberated PSF of the (pre-COSTAR) HST, in combination with the large science aperture (LSA) of the GHRS, results in a spectral point spread function consisting of a narrow ($\sim$ 16 km s^{-1}) core and a 60 km s^{-1} wide halo. This, of course, is a considerable degradation relative to the nominal resolution of the G160M grating which should be about 11.5 km s^{-1} (Duncan 1992). On the other hand, using the small science aperture would have involved a considerable loss of light, which we considered unacceptable in view of the faintness of our targets. As will be shown in the later sections, the choice of the LSA provides us with sufficient signal to noise to detect and analyze weak – hot gas – absorption lines.

Other observational parameters are the use of the default substep pattern 4, as well as the standard FP-split. The so-called comb-addition was used to reduce the effects of the fixed pattern noise of the Digicon diode array. On-board Doppler compensation, which corrects for the orbital motion of the spacecraft, was working correctly during all our integrations. The wavelength calibration was improved using spyballs as described in the HST data handbook.

The spectra were resampled to a linear wavelength scale with 0.0355 Å pixel^{-1} for the spectral region of the Si II line and 0.0345 Å pixel^{-1} for the spectral region of the C IV doublet. Figure 2 shows the spectra; the S/N at the continuum level in each spectrum is given in Table 2.

The spectra were normalized by fitting Legendre polynomials to the continuum. The steeply rising part of the strong stellar P Cygni profiles had to be fitted independently from the other parts of the spectra. In these subregions Legendre polynomials, also fitted with the IRAF 'continuum' again gave a tight fit to the stellar continuum. Fig. 3 shows the profiles of the interstellar lines after normalization.

Table 2. Data on the GHRS spectra

Star	λ_c	$t_{\rm int}$[s]	S/N	$v_{\rm rad}$(LSR)
Sk −67 169	1305 Å	1305.6	24	+258
Sk −67 169	1550 Å	6528.0	38	
Sk −66 118	1305 Å	435.2	14	+275
Sk −66 118	1550 Å	2176.0	24	

The IUE spectra were obtained in full shift exposures from VILSPA, three spectra were taken from the IUE archive. The relevant data are given in Table 3. The spec-

Table 3. Data on the IUE spectra

Star	SWP	$t_{\rm exp}$[m]	Observer
Sk −66 117	27896	361	de Boer & Koornneef
Sk −66 118	28100	380	de Boer & Koornneef
Sk −67 206	27888	308	de Boer & Koornneef
Sk −67 169	43299	380	Bomans
	44362	406	Bomans
Sk −66 100	31339	850[a]	Garmany
Sk −67 166	6967	240[a]	Conti
	8011	255[a]	Stickland

[a] taken from IUE archive

tra cover the wavelength range of about 1150 Å to 2000 Å. The basic reduction of the spectra was done with standard routines at the IUE observatory and the spectra were further processed in Bonn using MIDAS. This included rebinning, slight filtering of the oversampled data to reduce the noise, and transformation to a velocity scale. Part of the IUE data has been presented in a study of the dynamics of the neutral gas in LMC 4 (Domgörgen et al. 1995). In 1986, a spectrum of Sk −66 117 at about 5′ from Sk −66 118 was also obtained; this spectrum turned out to be much weaker then we expected, and the achieved S/N ratio does not justify an analysis of the absorption features.

3. Stellar lines

In addition to the interstellar absorption features that are the primary focus of our present investigation, both the spectral regions we observed with the HST-GHRS contain strong stellar lines. The spectral region around 1550 Å is dominated by the P Cygni profile of the C IV doublet, while in the spectral region around 1300 Å strong absorption lines of particularly Si III (1294.543, 1296.726, 1298.891+1298.960, 1301.146, 1303.320 Å; see e.g. Wollaert et al. 1988) are present, as visible in Fig. 2. These stellar lines in our HST spectra can be used for a spectral classification independent of the one given in Domgörgen et al. (1995), based on high dispersion IUE spectra of relatively low S/N, and the optical classification from the literature. The strength of the stellar lines observed in our HST spectra appear to agree with the classification listed in Domgörgen et al. (1995), confirming a higher temperature for Sk −67 169 than for Sk −66 118.

Using the 5 strong Si III lines around 1300 Å we determined the radial velocity of our target stars. The results are 258±5 km s^{-1} for Sk −67 169 and 275±7 km s^{-1} for Sk −66 118. The uncertainty given here is the internal uncertainty of the measurement. The actual error may be slightly higher due to the blending of the galactic component of the interstellar O I and Si II with the two highest wavelength Si III lines and residual effects of the wavelength calibration of the spectra using the GHRS spyballs.

The derived radial velocities are typical for LMC stars in the field of supergiant shell LMC 4. The radial velocity of Sk −66 118 coincides with the velocity of a broad H I emission component at this position (Domgörgen et al. 1995). The radial velocity of Sk −67 169 is 20 km s^{-1} lower than the H I components listed in Domgörgen et al. (1995), but coincides with interstellar absorption components found in the IUE spectra of this star.

4. The low ionized gas

Interstellar absorption by O I and Si II is clearly detected in the spectra of both stars over a velocity interval from 30 to 150 km s^{-1}, while the wings to negative velocities (−30 km s^{-1}) are probably the effect of a blend with stellar Si III lines. The interstellar absorption components in the above velocity range belong most probably to the galactic halo (Savage & de Boer 1981, de Boer et al. 1990), and are known since the first IUE observations of LMC stars (Koornneef et al. 1979). Additional strong absorptions in O I and Si II are seen at velocities between 200 and 330 km s^{-1} and are associated with interstellar gas belonging to the LMC (see e.g. de Boer & Savage 1980 and Domgörgen et al. 1995).

The weak interstellar line of Ni II at 1317 Å is not convincingly detected in our spectra. While the spectrum of Sk −66 100 shows two weak dips at about the right velocity for the two dominant LMC components visible in O I and Si II, absorption at galactic velocities only consists of a broad, weak depression in the continuum without clear indication of narrow interstellar absorption components. From the IUE data we know that the column density of galactic gas is at least comparable to the LMC column densities. In view of the known lower metal abundance of the diffuse gas in the LMC (e.g. de Boer et al. 1987) the two weak spectral structures at LMC velocity are unlikely to be Ni II detections. In the spectrum of Sk −66 118 no Ni II absorption is visible at LMC velocities. At velocities compatible with galactic disk and halo gas, two weak dips are visible on top of a gentle depression of the continuum. Again, comparison with the absorption strength of the Si II and O I lines casts doubt on the reality of the lines. The halo components are generally located on the linear part of the curve of growth, therefore their strength is linearly correlated with the column density. The Ni II lines at halo velocities (if they are real) are much stronger than at galactic disk velocities. This would imply Ni II overabundance in the halo clouds along this line of sight, a highly improbable situation. More probable is a stellar Ni II line of this relatively 'cool' B2 star.

C I is present in our spectra over the full velocity range (0 to 300 km s^{-1}) in each line, but the limited spectral resolution of (pre-COSTAR) GHRS does not allow us to disentangle C I and the 4 excited C I lines in this spectral region.

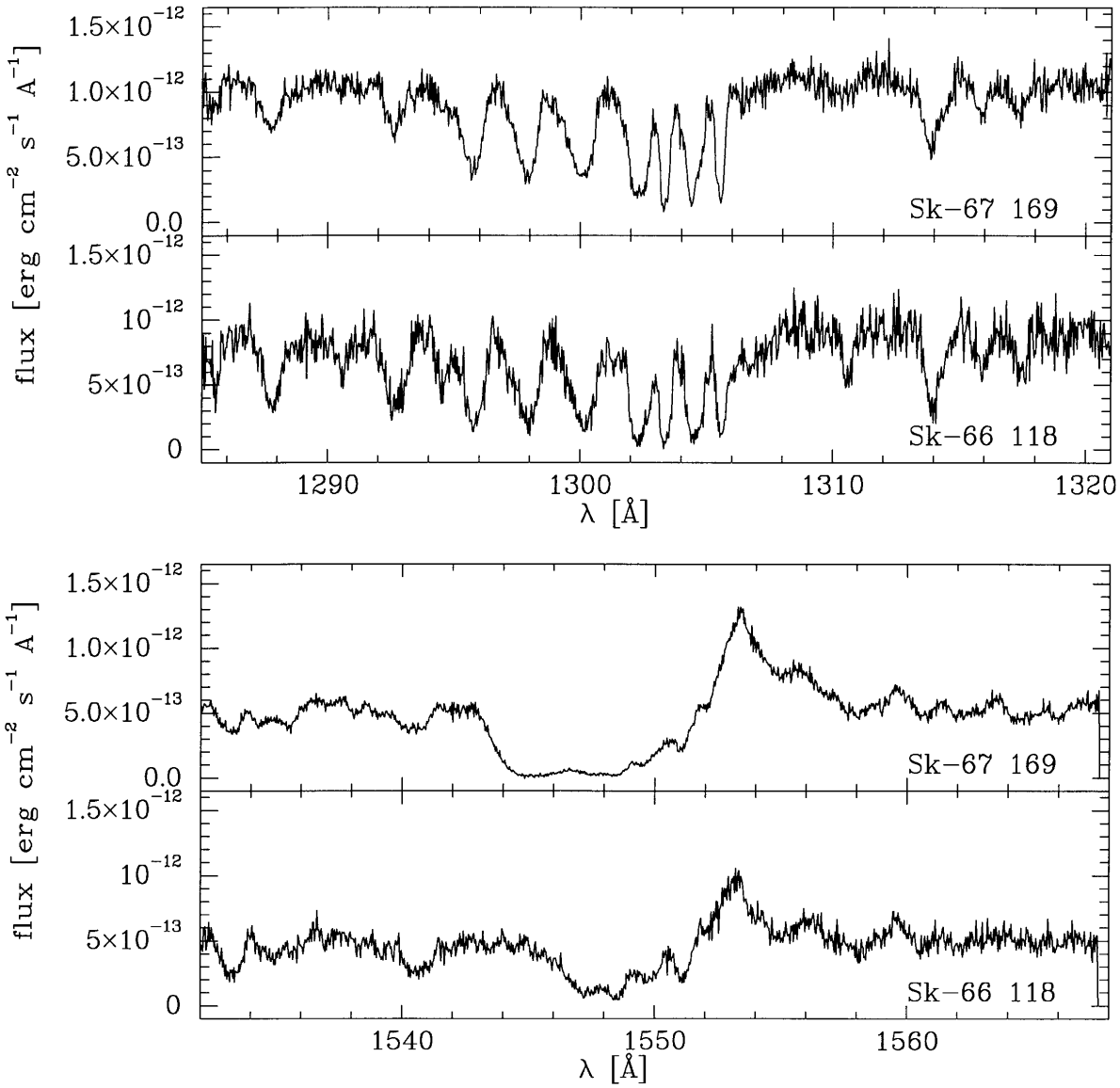

Fig. 2. Spectra obtained with the HST for Sk −67 169 and Sk −66 118 are shown for the wavelength ranges 1285 to 1321 Å and 1532 to 1568 Å. Here the strong stellar Si III lines (1294.543, 1296.726, 1298.891+1298.960, 1301.146, 1303.320 Å) and the C IV P Cygni like line (centered at 1549 Å) can be recognized. The sharper structures are due to interstellar absorption lines of O I, Si II, and Ni II in the former wavelength range and due to the C IV doublet in the latter wavelength range. Note that the interstellar absorptions are double due to galactic gas near 0 km s^{-1} and to LMC gas near 270 km s^{-1} (LSR).

The two lines of excited states of O I at 1304.86 and 1306.03 Å are not detected in our spectra.

5. Interstellar C IV

The stellar C IV P-Cygni profiles prominently visible the two lower panels of Fig. 2 show significant spectral structure which is due to interstellar absorption indicating narrow absorption lines superimposed on the smooth stellar continuum. After fitting the steeply rising continuum (see Sect. 2), four narrow interstellar absorption components are nicely visible (Fig. 3). Their central wavelengths correspond to two components of the C IV doublet each with the galactic and LMC gas velocity structure. For Sk −67 169 the central absorption velocities are 57 and 270 km s^{-1}, while for Sk −66 118 the features are centered at 63 and 280 km s^{-1}. The strong absorption near 60 km s^{-1} is known to be due to hot gas in the halo of the Milky

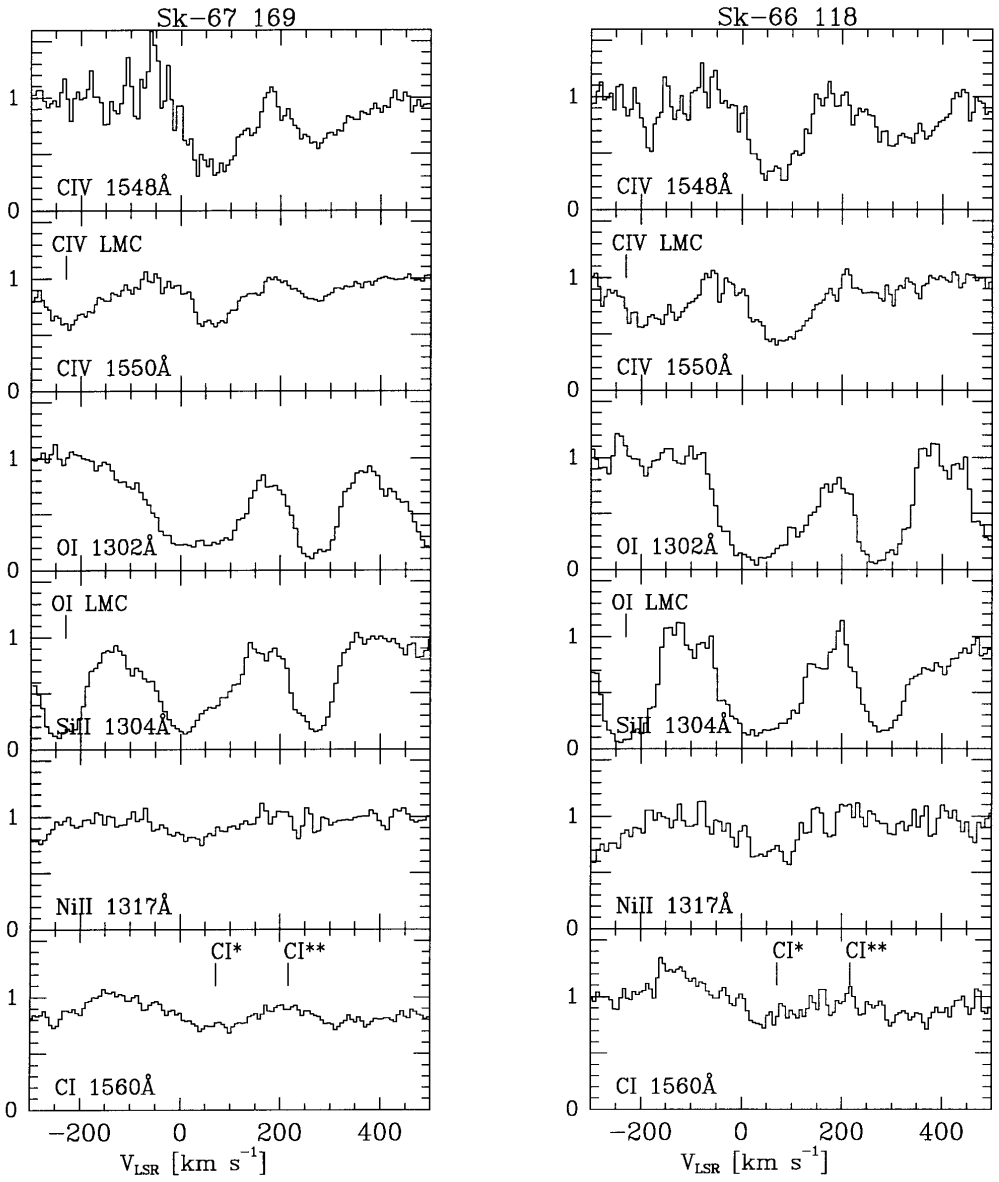

Fig. 3. The interstellar absorption lines present in the HST spectra have been normalized to the stellar continuum and are plotted against velocity (LSR), with from top to bottom O I 1302.168, Si II 1304.370, Ni II 1317.217, and the two lines of the C IV doublet at 1548.195 and 1550.770 Å. Note the absorption due galactic gas between −50 and +180 km s^{-1} and by LMC gas between +200 and +350 km s^{-1}. The strong noise at low velocity in the C IV 1548 profiles results from the very low stellar background flux in the absorption component of the stellar P Cygni profile.

Way (Savage & de Boer 1981). We associate the absorptions near the systemic velocity of the LMC with hot gas inside the supergiant shell LMC 4.

We will make the analysis of the C IV lines in 3 steps. First, we will investigate the equivalent widths of the absorbing components (see below). An analysis of the actual profiles in terms of velocity dependent optical depth follows (Sect. 5.2). Finally, we apply a deconvolution-reconstruction algorithm to the spectra, taking into account the actual PSF of the GHRS. The optical depth analysis of Section 5.2 is then repeated for these 'sharpened' spectra, and the results compared. Since this procedure requires a fairly elaborate discussion, it is presented in a separate section (Sect. 6).

5.1. C IV equivalent widths and column densities

Under the simplifying assumption that the observed equivalent widths are due to a single Galactic plus a sin-

gle LMC component, we can determine their C IV column densities using the curve of growth approach.

The LMC absorptions have equivalent widths of about 80 mÅ and 200 mÅ for the two lines of the doublet, which is close to the theoretical – optically thin – ratio of two for these lines. In the optically thin approximation, the equivalent widths translate readily into C IV absorption column densities of $N(\mathrm{C\,IV}) = 5\ 10^{13}$ cm^{-2} for both lines of sight.

In contrast, the two galactic halo absorption components are about equally strong (300 mÅ) and are therefore saturated. Thus, only a lower limit for the column density of these high ions can be found, with $N(\mathrm{C\,IV}) > 10^{14}$ cm^{-2}. Note, however, that this result suffers some additional uncertainty due to the location of the galactic component of the C IV line at 1548 Å near the bottom of the stellar C IV absorption line.

The applicability of the curve of growth method is severely limited if an apparently optically thin observed profile actually consists of narrow and unresolved components, which individually could well be significantly saturated. For this case, the 'apparent optical depth' approach offers some relief, and we now discuss the results of this method.

5.2. C IV column densities from apparent optical depth

If an observed absorption profile shows spectral structure, we can apply the velocity resolved optical depth method (e.g. Sembach & Savage 1992). In this method, the data points of the observed line profiles are converted to apparent optical depth:

$$\tau_a(v) = ln\left(\frac{I_{cont}(v)}{I_a(v)}\right), \qquad (1)$$

and thereafter to apparent column density:

$$N_a = \left(\frac{m_e c}{\pi e^2}\right)\frac{1}{\lambda f}\ \tau_a \ \ [\mathrm{atoms\ cm^{-2}\ (km\ s^{-1})^{-1}}]. \qquad (2)$$

Fig. 4 shows the apparent optical depth profiles for the spectral region around the C IV lines.

The condition that the narrowest intrinsic structure of the spectral line is fully resolved is, at a GHRS resolution of about 11 km s^{-1} not necessarily fulfilled for lines due the low ions. As is well known (see e.g. ζ Oph, de Boer & Morton 1974), such absorptions may be due to clouds with b-values as small as 1 km s^{-1}.

However, for the absorptions of C IV the direct transformation from absorption depth into optical depth is valid since the C IV ion exists normally only in gas of temperatures above 10^5 K. The thermal width then exceeds about 20 km s^{-1}. Only if the C IV ions were to exist in gas which has cooled down to 10^4 K without having recombined (in the case of rapid adiabatic expansion, which 'freezes' the ionizational structure; e.g. Breitschwerdt & Schmutzler 1994) could the intrinsic structures be narrower (see next section).

For Sk −67 169 the profiles of the two lines agree with each other to within the errors, implying no hidden saturated components. Decomposing the profile in components, the C IV column density can therefore be accurately determined to 1 10^{14} cm^{-2} for the 70 km s^{-1}, 1.5 10^{13} cm^{-2} for the weak 140 km s^{-1} component, and 6 10^{13} cm^{-2} for the 270 km s^{-1} component.

For Sk −66 118 the situation is different. The optical depth profile clearly indicates saturation over most of the velocity range, but in particular for the component of the galactic halo at about 70 km s^{-1} limiting the column density determination there to a lower limit of 1 10^{14} cm^{-2}. For the LMC component the somewhat lower S/N in this spectrum becomes a factor, but it is nevertheless clear that in some parts of the profile unresolved, saturated components are present. Therefore the C IV column density for the LMC part of the line-of-sight derived from the Sk −66 118 spectrum of 6 10^{13} cm^{-2} is somewhat uncertain and probably has to be interpreted as lower limit.

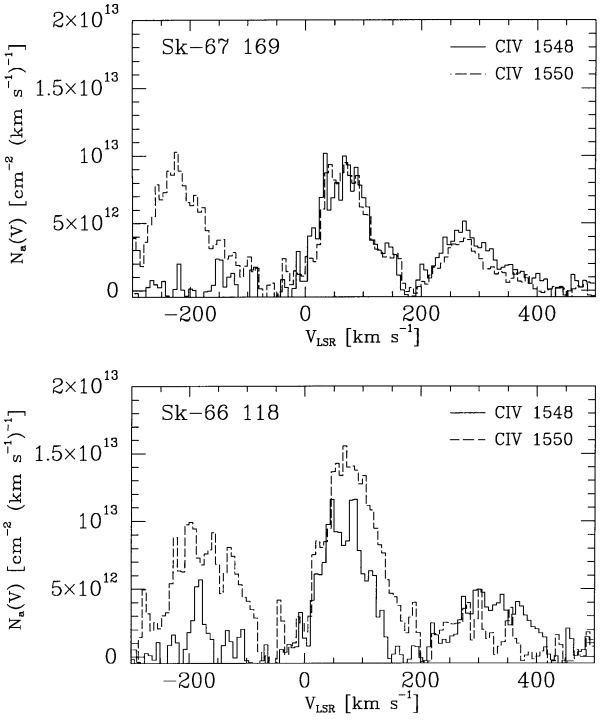

Fig. 4. The absorption seen in the C IV lines of Fig. 3 is transformed into apparent optical depth profiles and after appropriate conversion the column density profile is obtained as shown. In those locations where the column density profile, $N(v)$, of the 1548 Å line deviates from that of the 1550 Å line, saturation is present in the stronger of the two lines.

6. Spectral Restoration

While the interstellar absorption lines of interest are clearly visible in our spectra, their velocity structure (as indicated from our IUE high dispersion spectra of these stars) is compromised by the asymmetric line spread function of the pre-COSTAR GHRS. As the signature imposed by the GHRS on the observed spectra is well known and temporally stable, the intrinsic spectral line profiles can be recovered to some extent. Not only are we interested in achieving a match to the intrinsically narrowest lines, but we would also like to know whether the broad wing to higher velocities seen in the line profile of the component at LMC velocity is real or due to the line spread function (LSF) of the telescope-spectrograph combination.

To recover some of the spectral resolution, and to make optimal use of the high S/N in our spectra, we used a modified Lucy algorithm with entropy constraint (Walsh & Lucy 1993) to deconvolve our spectra. The method conserves the flux, while the entropy constraint helps to keep the noise from amplifying. However, finding a balance between an optimal sharpening and generating unphysical, spurious, spectral structure remained the major challenge.

We made several runs with different parameters. The results we liked best were obtained with 30 iterations and a very small entropy constraint. We used for this process exclusively the data of Sk −67 169, because the spectra have a much higher signal to noise ratio. Initial tests with the Sk −66 118 spectra showed that for these datasets the resolution gain is not outweighed by the much higher noise level. Scientifically, this a not a big loss, because we determined already in Section 5.2 that the interstellar C IV absorption lines in Sk −66 118 are saturated, and they will thus not show additional structure at higher spectral resolution.

Figure 5 shows the results of the restoration process in comparison to the original data of Sk −67 169. Normalization was done for both data sets in the same way as described in section 2.

The interstellar absorption lines are much better defined in the deconvolved spectra, clearly showing a gain in spectral resolution, especially by correcting for the broad wings of the LSF. The line profile of Si II provides a good example. The actual spectral resolution is difficult to determine, because in our spectra no isolated, narrow interstellar line is present; using the only slightly blended lines it can be estimated to be about 16 km s^{-1}. This value is very close to the theoretical limit given by the width of the LSF core (Duncan 1992).

6.1. Low ionization stage lines

The velocity structure of the neutral gas as traced by Si II can now be interpreted as corresponding to interstellar clouds at 20, 65, 110, 250 and 290 km s^{-1}. In the IUE spectra these components were also found (see e.g. Domgörgen et al. 1995), except that the two components at 275 and 300 km s^{-1}claimed there merge into a single component near 290 km s^{-1} in the HST spectra. The difference is likely due to the higher S/N in the HST spectra.

The velocity pattern from the O I line agrees reasonably well with that from Si II for the galactic components, having radial velocities of 20, 70, and 100 km s^{-1}. At LMC velocities a slightly different pattern is visible with absorption components at 260 and 305 km s^{-1}. This may indicate that the 300 km s^{-1} component in the IUE spectra has a higher column density in O I than in Si II. One possible explanation for this difference could lie in a variation of elemental abundances due to different depletion into dust grains, which could occur if these velocity components correspond to spatially distinct interstellar environments (i.e., inside or outside supergiant shell LMC 4 respectively). Clearly much more data would be needed to test this speculation.

The broad depression of the continuum of the Ni II line at 1317 Å is now resolved into the principal velocity components at galactic velocity. At LMC velocity still no Ni II is convincingly detected.

6.2. The C IV absorption in Sk −67 169

The largest gain from the deconvolution process is visible in the C IV lines. The high-velocity wing is transformed into a weak additional absorption component and the main absorption dip is now a nice, symmetric, single component profile. This shows clearly that the high velocity wing was an artifact of the line spread function of the pre-COSTAR HST-GHRS instrument.

Following the procedure given earlier, we converted the deconvolved spectrum into apparent optical depth, and then calculated the apparent column density profiles. These profiles are given in Fig.6. The velocity components of the C IV line can now be traced as 35, 73, 145, 277, and 318 km s^{-1}. We must note that the relatively poor signal to noise in the C IV 1548 profile is the result of the location of this line near the bottom of the stellar C IV P-Cygni profile of Sk −67 169.

The galactic 35 km s^{-1} is somewhat uncertain due to low S/N, but if real, then the line is saturated. For all other components the profiles of the two C IV lines agree well, therefore accurate column densities can be derived by integrating the apparent column density profile in the velocity intervals of the components. Table 4 shows the results, which agree well with the results of the integration of the raw spectrum and the curve-of-growth results, proving that the spectral restoration did not significantly affect the flux scale. When comparing the column densities one has to keep in mind that due to the spectral restoration more components could be measured individually as result of the resolution of the broad profiles in the unprocessed spectra.

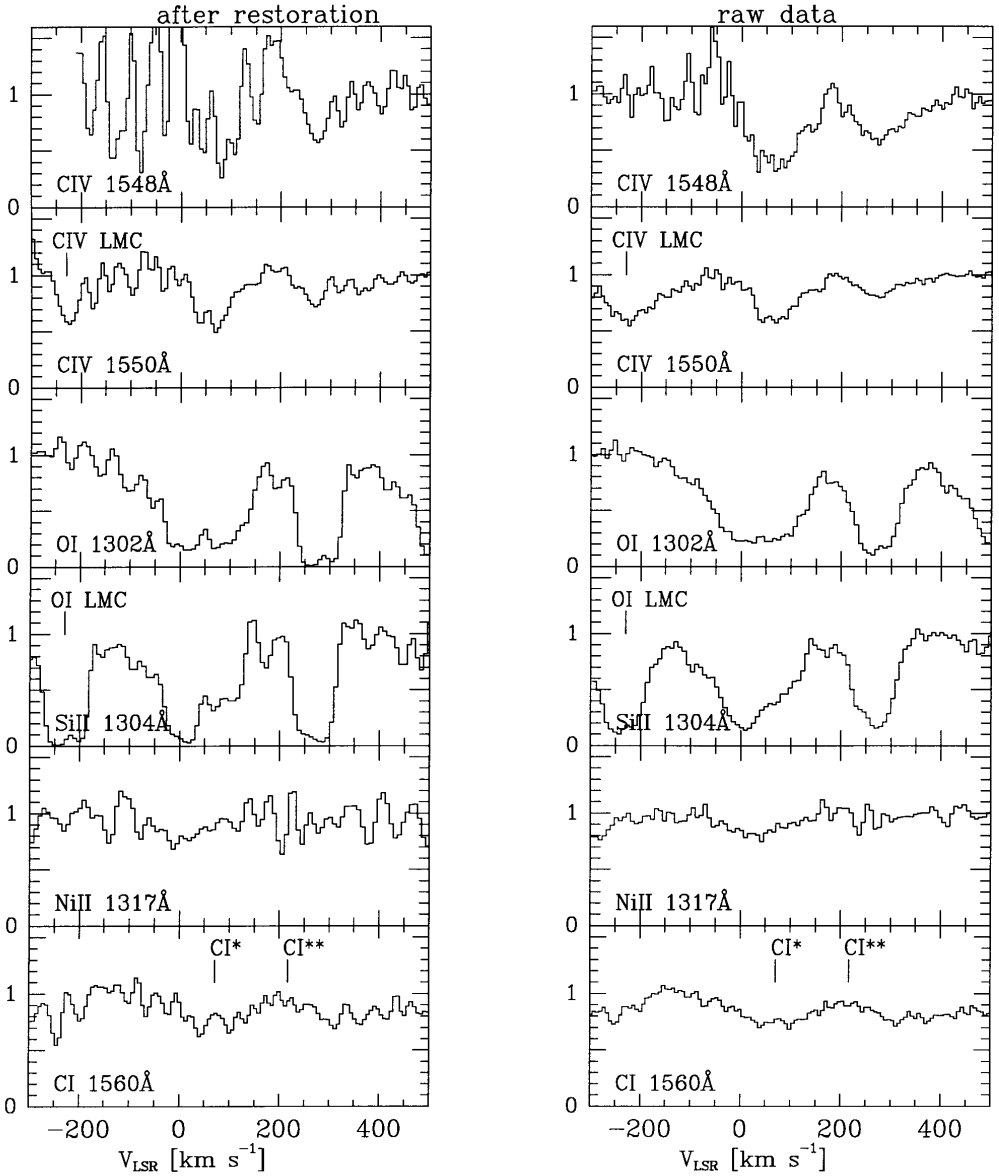

Fig. 5. Interstellar line profiles in the Sk −67 169 spectra **after** and before application of the resolution restoration routine.

The galactic C IV component at 73 km s^{-1} agrees well in velocity and column density with the results of Savage & de Boer (1981) toward other LMC stars. The C IV column densities and velocities of this absorption component on the two lines of sight (which are 17′ apart) indicate that the origin of this component is located in the halo of our Galaxy and not in the LMC. At the distance of the LMC the absorbers would have to be one cloud with a diameter larger than 250 pc to produce these very similar absorptions on our two lines of sight. A cloud in the halo of our galaxy is an order of magnitude closer in space and the apparent homogeneity is then expected. A weak component at 110 km s^{-1} is not well resolved in the restorated spectrum of Sk −67 169, but seems to be present in both lines of the C IV doublet. We therefore do not give a individual column density of the component. The same comments about the physical location as for the 73 km s^{-1} component apply.

The 145 km s^{-1} C IV component on the line of sight to Sk −67 169 has no counterpart in the spectrum of Sk −66 118. One possibility is that this is an additional small high-velocity cloud (HVC) only intercepted on one line of sight. Similar velocities are known in the general area (see de Boer et al. 1990). However, contrary to the two well known HVCs at about 60 and 130 km s^{-1} this

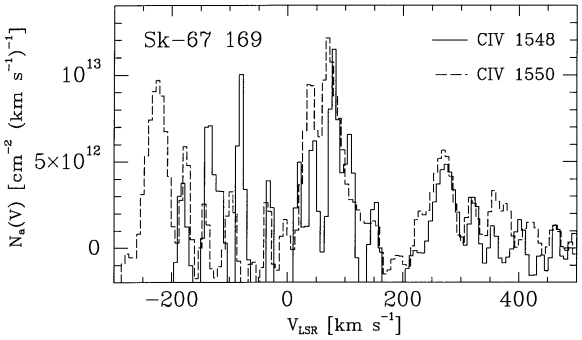

Fig. 6. Apparent column density profiles of the C IV of Sk −67 169 AFTER application of the resolution restoration software.

C IV absorption component has no counterpart in Si II and O I.

The two C IV components at LMC velocity are well resolved now, which enable us to use the actual profiles of the absorptions to derive additional information. The stronger absorption at 277 km s^{-1} is symmetric and has a full width at half maximum of 40 km s^{-1} (39 km s^{-1} for C IV 1548 and 41 km s^{-1} for C IV 1550). This is much larger than the spectral resolution defined by the core of the LSF (11.5 km s^{-1}; Duncan et al. 1992). Even if we did not recover the full intrinsic spectral resolution of the GHRS G160M grating, our estimated resolution of 16 km s^{-1} implies that this 277 km s^{-1} component is easily resolved.

We can now use the line width to derive a kinetic temperature of the absorbing C IV gas, if we assume pure thermal broadening. The full width half maximum, FWHM, is given by

$$FWHM = 2\sqrt{ln\ 2}\ \sqrt{\left(\frac{2\ k\ T}{m}\right)} \qquad (3)$$

and therefore

$$FWHM = 0.215\ \sqrt{\frac{T}{A}}\quad [\mathrm{km\ s^{-1}}] \qquad (4)$$

with temperature T, the mass of the atom m, the Boltzmann constant k, and the atomic mass number A (Savage 1987). For 10^5 K, the temperature of the peak ionic abundance under thermodynamic equilibrium (e.g. Shull & van Steenberg 1992), the C IV absorption lines would have a width of 20 km s^{-1}. To this we must add the effect of the smearing due to the instrumental profile (16 km s^{-1}, see above), near C IV bringing the total width to 27 km s^{-1}. The observed C IV component at 277 km s^{-1}, if interpreted as due to such thermal gas, would imply a plasma of 1.4 10^6 K. At this temperature the ionic abundance of C IV would be low. The observed width therefore must mean that the gas is either in non-equilibrium conditions or a that the line width has a non-thermal origin, such as blending of components or velocity gradients. A detailed discussion of the C IV results will be given in Sect. 9.

Table 4. C IV column densities

Star	$v_{\mathrm{LSR,C\,IV}}$	$N_{\mathrm{C\,IV,r}}$	$N_{\mathrm{C\,IV,d}}$
Sk −67 169	35	1 10^{14}	$> 2\ 10^{13}$
	73		6 10^{13}
	145	1 10^{13}	7 10^{12}
	277	6 10^{13}	3 10^{13}
	318		6 10^{12}
Sk −66 118	73	$> 1\ 10^{14}$	
	130	$> 3\ 10^{13}$	
	280	6 10^{13}	

Notes: r, from raw spectra; d, from deconvolved spectra

7. Profile fitting

An alternative way to analyze the profiles of interstellar lines observed with GHRS before COSTAR is described in Lu et al. (1994). They fitted their spectra with Voigt profiles which were smeared with the aberated PSF. We used the MIDAS context CLOUD for the same process and used the the line spread function given by Duncan (1992). Because the spectra of Sk −67 169 have clearly better signal to noise ratio and the lines are not all saturated, we used only this object.

The fit supports the results from the deconvolution: after plotting a best fit one-component model over the spectrum the weak additional C IV component at 145 km s^{-1} clearly shows up. The high velocity wing of the C IV line turns out to be partly due to the instrumental profile and partly due to a real feature. We tried to make a fit with more than the three components for the galactic halo C IV and the two components for the LMC absorption. This did not work well, which may be an effect of slight deviations of the actual LSF of our observation from the standard LSF given by Duncan (1992). These differences can easily be induced by the target not being perfectly centered in the aperture. The results of the spectral restoration do not unambiguously allow more components into the fit.

8. The IUE spectra and comparison with HST

The spectra obtained with the IUE are of only very moderate signal-to-noise and have a spectral resolution equivalent to slightly more than 20 km s^{-1}. A detailed analysis of the velocity structure of the low ionized lines is given in Domgörgen et al. (1995).

While there are indications of interstellar C IV absorption in IUE high dispersion spectra to targets inside LMC 4 (Bomans et al. 1990, Domgörgen et al. 1993), the

interpretation is severely limited by the low S/N of the available IUE high dispersion spectra. Sk −66 117 and also Sk −66 118 have been dropped for the analysis, because the spectra turned out to be too noisy. Table 4 shows the results. The most convincing detection is in the spectrum of Sk −67 166, with $N(\mathrm{C\,IV}) = 5.0\ 10^{13}$ cm^{-2} at a velocity of 270 km s^{-1}. Sk −67 166 is unfortunately an O6 star, and a significant amount of the detected C IV may be due to ionization of the circumstellar surroundings by the star itself. This circumstellar contribution needs more detailed analysis before any conclusions can be derived from this interesting line of sight. The same is true for the line of sight to Sk −66 100. HST observations of such hot stars and detailed modeling of the circumstellar contribution of the star will be presented elsewhere. The other IUE spectra give upper limits for the C IV column density in agreement with our detections presented in this paper.

Due to the large spectral range covered by a SWP spectrum of the IUE, additional information can be derived from the Si IV and N V doublets at 1400 and 1240 Å. Results are collected in Table 5.

Si IV is possibly detected but only in the weaker line of the doublet. This is similar to the situation of C IV in the HST spectra, where the stronger line of the P Cygni doublet leaves too little signal for a clear detection of the superimposed interstellar absorptions. However, the velocity of the dip is 260 km s^{-1}, about 20 km s^{-1} lower than the C IV absorption in the HST spectrum. Additionally, 260 km s^{-1} is exactly the stellar radial velocity of Sk −67 169, which implies that the Si IV absorption line probably originates in the circumstellar environment of this B1 star. The association of the Si IV absorption with that of C IV is therefore very questionable and no temperature for the interstellar hot gas on the Sk −67 169 line of sight can be derived from this ratio.

Assuming equilibrium electron collisional ionization and solar abundances we can use the calculations of Shull & van Steenberg (1982) together with the observed column densities to estimate the gas temperature. For Sk −67 169, using the C IV column densities from the HST spectrum and the limits for Si IV and N V derived from the IUE spectrum, we get $N(\mathrm{C\,IV})/N(\mathrm{Si\,IV}) \sim 0.5$ and $N(\mathrm{N\,V})/N(\mathrm{C\,IV}) \leq 5$.

The limit for the N V to C IV ratio is very high, consistent with a temperature of less or equal to $1\ 10^6$ K, in agreement with a thermal interpretation of most of the C IV line width.

9. Discussion

We have found substantial column densities of C IV in the direction of stars inside the supergiant shell LMC 4. The C IV absorption is seen at 277 km s^{-1} for the stronger component. This velocity is marginally smaller than that of the bulk material (stars and neutral gas) of LMC 4 having $v_{\mathrm{LSR}} = 287$ km s^{-1} (see Domgörgen et al 1995).

Table 5. Column densities of high ions detected in IUE spectra at $v_{\mathrm{rad}} \sim 260$ km s^{-1}

Star	N(Si IV)	N(C IV)	N(N V)
Sk −67 169	$4.0\ 10^{13}$	$\leq 2.0\ 10^{14}$	$\leq 1.5\ 10^{14}$
Sk −67 206	$\leq 1.5\ 10^{13}$	$\leq 6.0\ 10^{13}$	$\leq 1.0\ 10^{14}$
Sk −67 166		$5.0\ 10^{13}$	
Sk −66 100		blemish	

From the lack of C IV gas in the velocity range between 250 and 200 km s^{-1} on both lines of sight we can conclude that a blow-out of LMC 4 into the LMC halo has, at present, probably not taken place at the front side of LMC 4.

The observations of absorption lines from gas inside the superbubble have a topographical bias; since we do not know at what depth the stars lie inside LMC 4 we more likely sample gas of the near side of the superbubble. The detected velocities indicate therefore that the C IV gas is coming toward us. If we assume that the gas comes from a mixing layer (e.g. Slavin et al. 1993) between X-ray emitting gas inside LMC 4 and the cool shell, then the superbubble is still expanding with a very small velocity of about 10 km s^{-1}, well fitting to the results of Domgörgen et al. (1995) for the front side of LMC 4. In this case the large width of the line would rather be explained by turbulent motions in the conducting interface than by thermal broadening.

The other possibility for the origin of the 280 km s^{-1} C IV absorption is the interior of LMC 4 itself. Interpreting the line-width as purely thermal the resulting temperature of $1.4\ 10^6$ K agrees within the errors very well with the temperature of the X-ray emitting plasma inside LMC 4 having a temperature of $2.4\ 10^6$ K (Bomans et al. 1994).

Depending on the location of the stars inside LMC 4, we can derive an average gas density of C IV. With a column density $N(\mathrm{C\,IV}) = 6\ 10^{13}$ cm^{-2}, the average density of C IV for a 1 kpc column (star at the rear side of LMC 4) or for a 500 pc column (star at the center of LMC 4) is $n(\mathrm{C\,IV}) = 2$ or $4\ 10^{-9}$ cm^{-3}, respectively. At the temperature of the peak ionic abundance of C IV and the metallicity of the LMC this corresponds to $n_{\mathrm{H}} = 1\ 10^{-4}$ cm^{-3}. For the temperature of $2\ 10^6$ and LMC metallicity this corresponds to less than $1\ 10^{-8}$ cm^{-3} in H. The average density of the hot gas derived from ROSAT data of $n_{\mathrm{e}} = 8.0\ 10^{-3}$ cm^{-3} effectively excludes the high temperature implied by a thermal interpretation of the line width because the observed C IV column density is larger by orders of magnitudes. We can therefore conclude that the line width of the C IV line is at least partly due to bulk motions of C IV clouds.

The other result of the crude estimation is that, even at the temperature of the peak ionic abundance of C IV, the filling factor of C IV is smaller than that of H. This again supports an origin of the the C IV absorption from

clouds inside LMC 4 and from a conducting layer on the front side of the expanding supergiant shell. The filling factor will be even smaller, if we assume that the hot gas inside LMC 4 is not at LMC abundance of about 1/3 solar, but more metal enriched due to the supernova explosions inside the supergiant shell.

Using the density estimate for the conducting front hypothesis, it becomes clear that one layer of pc size would imply a density of the order of $n = 1$ cm^{-3}, which would lead to rapid cooling. Many layers along the line of sight seem to be a more realistic description.

Interestingly the column density of C IV is the same for both lines of sight, which (if the stars are at equal depth in LMC 4) may point to a common origin. This may be one large cloud or a large collection of randomly distributed small clouds.

In the course of the discussion above we found indications for a population of C IV clouds inside LMC 4. This may be a population of cool clouds which survived the passage of several shock-waves inside LMC 4, or even was created by the passage of these shock waves through a clumpy ISM (Ferrara & Shchekinov 1993). These clouds are pushed around randomly and will all have interfaces with the hot plasma, in which most of the C IV is produced. Some contribution of quiescently cooling gas (e.g. Slavin & Cox 1992) to the C IV column density will be present as well. In this scenario our lines of sight will intersect several of this C IV layers. The average velocity of the created line will be near to the rest velocity of the gas in the region of LMC 4, or maybe at somewhat lower velocity due to the LMC 4 depth sampling bias explained above. The line-width of the resulting C IV line would be dominated by the bulk motion of the clouds and not by thermal broadening.

If these clouds (i.e. the mixing layers) are abundant inside LMC 4, as implied by our data, this has strong implications for the evolution of supergiant shells, leading to a stronger cooling inside, which limits their age and therefore their size. The need for an additional energy source becomes much more severe. More lines of sight have to be sampled to investigate the size and the filling factor of these C IV producing clouds to ensure that our two examples are not exceptional.

The second C IV component visible in both lines of sight, either as wing to high velocities or as second component (apparent after deconvolution) has to have a different origin because of its large velocity difference to the rest velocity at this location of the LMC. Its velocity is also higher than any velocity component of low ionized or neutral gas seen in absorption in our spectra. This excludes the possibility that this gas is related to the rear side of LMC 4, which appears to blow out into the halo of the LMC (Domgörgen et al. 1995). The high velocity gas appears to have similar velocity structure and column density in both observed lines of sight, as derived from the similarity of the high velocity wings in the not restorated spectra. This implies that the gas 'cloud' has an minimal size of 250 pc leading to large energy requirements independent of the actual 3-d structure. One possible explanation is that we detected a blast wave from a supernova which exploded inside the cavity of LMC 4. Such an event should lead to a faint, fast moving filament of enhanced emission (McCray 1988), describing the observation well. Interestingly, faint filamentary structure is also visible in the ROSAT images of LMC 4, which may have the same creation mechanism. Alternately the absorption could also be caused by a supernova fragment as proposed to exist in supergiant shells by Franco et al. (1993).

Based on early IUE spectra de Boer & Savage (1980) claimed that the LMC is surrounded by a hot halo, just like the Milky Way (Savage & de Boer 1981). The argument rested on the strengths of the C IV line and its velocity (see review of de Boer 1984). The velocity of the halo gas was near 220 km s^{-1}, a value much smaller that what we have detected toward LMC 4. In the HST C IV profiles one can see absorption extending down to about that velocity but no specific absorption component is present. In a recent paper, containing a detailed analysis of all archived and a significant number of new IUE high dispersion spectra of LMC stars, Wakker et al. (1996) show that there is no global corona of the LMC, but that a patchy one is still consistent with the data. Unfortunately from the present HST data we cannot derive further constraints about a hot corona of the LMC.

Acknowledgements. We thank Jeremy Walsh and Adeline Caulet at the ST-ECF for help during preparation of the phase two of the observations and with the basic steps of the HST data reduction. DJB likes to thank the ST-ECF staff for their hospitality during two stays at Garching. We thank especially Jeremy Walsh for letting us use his spectral restoration routines and for discussions about the handling of LSA data suffering from the aberated PSF. We thank You-Hua Chu and Mordecai Mac Low for comments and discussions.

DJB and EKG have been financially supported partly through the DFG Graduiertenkolleg 'Magellanic Clouds'. DJB thanks the Alexander von Humbold Foundation for support as part of their Feodor Lynen Fellowship program.

References

Boggess A., et 32 al., 1978, Nature 275, 372 & 377
Bomans D.J., 1994, PhD thesis, Rheinische Friedrich Wilhelms Universtität Bonn
Bomans D.J., de Boer K.S., Koornneef J., 1990, in: 'The Magellanic Clouds', eds. R. Haynes, D. Milne, IAU Symp. 148, Kluwer, p.436
Bomans D.J., Dennerl K., Kürster M., 1994, A&A 283, L 21
Bomans D.J., Vallenari A., de Boer K.S., 1995, A&A 298, 427
Breitschwerdt D., Schmutzler T., 1994, Nat 371, 774
Chu Y.-H., Mac Low M.-M., 1990, ApJ, 365, 510
Chu Y.-H., Wakker B., Mac Low M.-M., Garcia-Segura G., 1994, AJ 108, 1696
Cohen R.S., Dame T.M., Garay G., Montani J., Rubio M., Thaddeus P., 1988, ApJ 331, L 95

Conti P.S., Garmany C.D., Massey P., 1986, AJ 92, 48
de Boer K.S., 1984, in: 'The Magellanic Clouds', eds. S. van den Bergh, K.S. de Boer, IAU Symp. 108, Reidel, p. 375
de Boer K.S., Morton D.C., 1974, A&A 37, 305
de Boer K.S., Nash A.G., 1982, ApJ 255, 447 and 261, 747
de Boer K.S., Savage B.D., 1980, ApJ 238, 86
de Boer K.S., Koornneef J., Savage B.D., 1980, ApJ 236, 769
de Boer K.S., Jura M.A., Shull J.M., 1987, in: 'Scientific Accomplishments of the IUE', eds. Y. Kondo et al., Reidel, p. 485
de Boer K.S., Morras R., Bajaja E., 1990, A&A 233, 523
Deul, E.R., den Hartog, R.H., 1990. A&A 229, 362
Domgörgen H., Bomans D.J., de Boer K.S., Koornneef J., 1993, in: 'New Aspects of Magellanic Cloud Research', eds. B. Baschek, G. Klare, J. Lequeux, Springer, Lecture Notes in Physics 419, p. 161
Domgörgen H., Bomans D.J., de Boer K.S., 1995, A&A 296, 523
Duncan D. 1992, 'GHRS Instrument Handbook, version 3.0', STScI
Ferrara A., Shchekinov Y., 1993, ApJ 417, 595
Franco J., Ferrara A., Różyczka M., Tenorio-Tagle, G., Cox, D.P., 1993, ApJ 407, 100
Fitzpatrick E.L., 1988, ApJ 335, 703
Goudis C., Meaburn J., 1978, A&A 68, 189
Hunter D.A., Hawley W.N., Gallagher J.S., 1993, AJ 106, 1797
Igumentshchev I.V., Shustov B.M., Tutukov A.V., 1990, A&A 234, 396
Kennicutt R.C., Hodge P.W., 1986, ApJ 311, 85
Koornneef J., de Boer K.S., Savage B.D., 1979, in 'The first year of IUE', ed. A.J. Willis, Univ. Coll. London, p.56
Lu L., Savage B.D., Sembach K.R., 1994, ApJ 426, 563
Mac Low M.-M., McCray R., Norman M.L., 1989, ApJ 337, 141
McCray R., 1988, in 'Supernova Remnants and the Interstelalr Medium', eds. R.S. Roger, T.L. Landecker, Cambridge Univ. Press, p.447
Meaburn J., 1980, MNRAS 192, 365
Rohlfs K., Kreitschmann J., Siegman B.C., Feitzinger J.V., 1984, A&A 137, 343
Savage B.D., 1987, in 'Interstellar Processes', eds. D.J. Hollenback, H.A. Thronson, Reidel, p.123
Savage B.D., de Boer K.S., 1981, ApJ 243, 460
Sembach K.R., Savage B.D., 1992, ApJS 83, 147
Slavin J.D., Cox, D.P., 1992, ApJ 392, 131
Slavin J.D., Shull J.M., Begelman M.C., 1993, ApJ, 407, 83
Shull J.M., van Steenberg M., 1992, ApJS 48, 95 & 49, 351
Suchkov A.A., Balsara D.S., Heckman T.M., Leitherer C., 1994, ApJ 430, 511
Vallenari A., Bomans D.J., de Boer K.S., 1993, A&A 268, 137
Wakker B., Chu Y.-H., Bomans D.J., 1996, AJ, submitted
Walborn N.R., 1977, ApJ 215, 53
Walsh J.R., Lucy L.B., 1993, in 'The restoration of HST images and spectra', eds. R.J. Hainisch, R.L. White, STScI, p.267
Wollaert J.P.M., Lamers H.J.G.L.M., de Jager C., 1988, A&A 194, 197

This article was processed by the author using Springer-Verlag LaTeX A&A style file *L-AA* version 3.